Time-resolved depolarization analysis of back-scattered light

Time-resolved depolarization analysis of back-scattered light

Ernesto Pini[a,b], Fabrizio Martelli[a], Diederik S. Wiersma[a,b,c], Alexander Gatto[d], Henrik Schäfer[d], and Lorenzo Pattelli[c,b,e]

[a]Department of Physics and Astronomy, Università di Firenze, Sesto Fiorentino, Italy
[b]European Laboratory for Non-linear Spectroscopy (LENS), Sesto Fiorentino, Italy
[c]Istituto Nazionale di Ricerca Metrologica (INRiM), Turin, Italy
[d]Sony Europe B.V., Stuttgart Technology Center, Stuttgart, Germany
[e]National Research Council – National Institute of Optics (CNR-INO), Sesto Fiorentino, Italy

ABSTRACT

Studying the depolarization rate of light emerging from a turbid medium holds promise for the non-invasive characterization of its single-scattering properties, with relevant application in the quality analysis of different specimens or for diagnostic purposes in the biomedical field, to name a few. However, irrespective of sample geometry, the dynamics of light depolarization takes place on a time scale of few ps, which is too fast for traditional detection methods. Here, we present experimental results on the time-domain evolution of the depolarization ratio of light that is diffusely reflected from a scattering medium, using linearly polarized fs pulses in an all-optical gating scheme. Time-resolved reflectance curves are recorded in the parallel and perpendicular polarization channels relative to the illumination beam, granting direct access to the depolarization rate. We demonstrate our experimental approach on a lipid emulsion, fitting the data with a polarized Monte Carlo simulation to retrieve the average particle size and scattering asymmetry factor using just two time-domain reflectance measurements in a semi-infinite geometry.

Keywords: multiple scattering, depolarization rate, time-resolved reflectance, optical gating, depolarization ratio

1. INTRODUCTION

Among several techniques commonly used to study radiative transport in turbid media, time-domain methods are particularly relevant as they can provide direct access to the dynamics of light propagation. An even richer picture is obtained when time-resolved techniques are also capable of resolving the progressive depolarization of scattered light as it emerges from the target medium.[1–3] This type of measurement, which can be challenging due to the very short time-scales involved, can indeed reveal important information down to the single-scattering level that would be difficult to obtain otherwise, especially in a reflectance configuration.

When a scattering sample is illuminated by an ultrashort pulse of laser light in a single state of linear polarization, the resulting back-scattered intensity $I(t)$ can be divided in a co-polarized (CoP) component $I_{\parallel}(t)$ and a cross-polarized (CrP) component $I_{\perp}(t)$ with respect to the incoming polarization state. The resulting decomposition is typically expressed in terms of the depolarization coefficients $d_{\parallel,\perp}$:

$$I_{\parallel,\perp}(t) = d_{\parallel,\perp}(t) I(t). \tag{1}$$

Typically, $I_{\parallel}(t)$ and $I_{\perp}(t)$ exhibit large differences during the early transient, which are progressively washed out at later times, before they eventually converge to the same decay rate. This is due to the fact that after a few scattering events, the polarization becomes equally distributed along both polarization channels as light

Further author information:
E.P.: E-mail: ernesto.pini@unifi.it
L.P.: E-mail: l.pattelli@inrim.it
Telephone: +39 055 457 2477

quickly loses memory of the original polarization state. For this reason, the dynamics of light depolarization in a disordered medium can reveal interesting properties of the sample, potentially down to the single scattering level.

A convenient figure of merit to describe the depolarization process is the Depolarization Ratio δ_{R},[4,5] which is defined as:

$$\delta_{\mathrm{R}}(t) = \frac{I_{\parallel}(t) - I_{\perp}(t)}{I_{\parallel}(t) + I_{\perp}(t)} = \frac{d_{\parallel}(t) - d_{\perp}(t)}{d_{\parallel}(t) + d_{\perp}(t)}. \tag{2}$$

A value of $\delta_{\mathrm{R}} = 1$ corresponds to a situation where the reflected light is perfectly polarized light in the co-polarized channel, and vice versa for $\delta_{\mathrm{R}} = -1$. Finally, $\delta_{\mathrm{R}} = 0$ means that light is equally distributed among both polarization channels, which is what we expect to find after a short transient for scattering media. The temporal evolution of the δ_{R} transient for backscattered light depends on several sample properties in addition to the transport mean free path l_{t}, including the single-scattering asymmetry factor g and the distribution of scatterer shapes and dimensions. A remarkable property of the δ_{R} as a physical observable, is its exact independence from absorption since any absorption contribution is expected to cancel out in the ratio for homogeneous and isotropic media.

Building on the results available for spherical Mie scatterers,[6,7] we developed an analysis method to investigate depolarization, which we demonstrate qualitatively in a simple particle sizing application. In the case of backscattered light, approximated expressions can be written for the time-resolved depolarization coefficients as:

$$d_{\parallel}(t) \simeq \frac{1 + 2\mathrm{e}^{-t/\tau_{\mathrm{p}}}}{2 + \mathrm{e}^{-t/\tau_{\mathrm{p}}}}, \tag{3}$$

$$d_{\perp}(t) \simeq \frac{1 - 2\mathrm{e}^{-t/\tau_{\mathrm{p}}}}{2 + \mathrm{e}^{-t/\tau_{\mathrm{p}}}}, \tag{4}$$

where τ_{p} is a time scale associated to the depolarization process, known as the depolarization time. These approximated relations are typically considered valid after a few scattering events, but before the complete depolarization of light.

Substituting (3) and (4) in equation (2), we get an approximated formula for the time-resolved depolarization ratio:

$$\delta_{\mathrm{R}}(t) \simeq \frac{2}{3\mathrm{e}^{\frac{t-t_0}{\tau_{\mathrm{p}}}} - 1}, \tag{5}$$

where t_0 is a temporal offset that is included to account for the fact that the depolarization process requires that at least one scattering even has occurred, which introduces a delay after light has entered the scattering medium.

The depolarization time can be expressed equivalently as a depolarization length $l_{\mathrm{p}} = \tau_{\mathrm{p}} v$, where v is the speed of light in the medium. In the case of spherical scatterers, and as long as the asymmetry factor remains below a certain threshold $g \leq 0.7$, the depolarization length is known to be proportional to the transport mean free path $l_{\mathrm{p}} \propto l_{\mathrm{t}}$ and inversely proportional to the asymmetry factor $l_{\mathrm{p}} \propto g^{-1}$.

2. METHODS

2.1 Experimental setup

The experimental setup is based on a series of laser sources producing two near-infrared synchronous pulses at a repetition rate of 80 MHz (Fig. 1). A CW diode laser (532 nm, 9.7 W) pumps a Ti:Sa laser (820 nm, 2 W), which in turn produces a train of ultrashort pulses with a typical duration of $\sim$ 150 fs. Each pulse goes through an Optical Parametric Oscillator, which outputs a down-converted signal (1525 nm, 150 mW) which we use as the optical gate, and an unconverted residual of the original beam (820 nm, 330 mW), which we use as the probe. Linear polarizers are used along both arms to further refine the linear polarization state of the beams, while half-wave plates allows complete control of the polarization orientation. The probe is focused on the sample at a small incidence angle $\alpha < 10°$, and the diffuse reflection signal is collected. A motorized delay line is used to control the relative delay between the two pulses with micrometric precision, resulting in a sub-ps time resolution. The two beams impinge onto a 2 mm-thick β-barium borate (BBO) non-linear crystal in a collinear geometry,

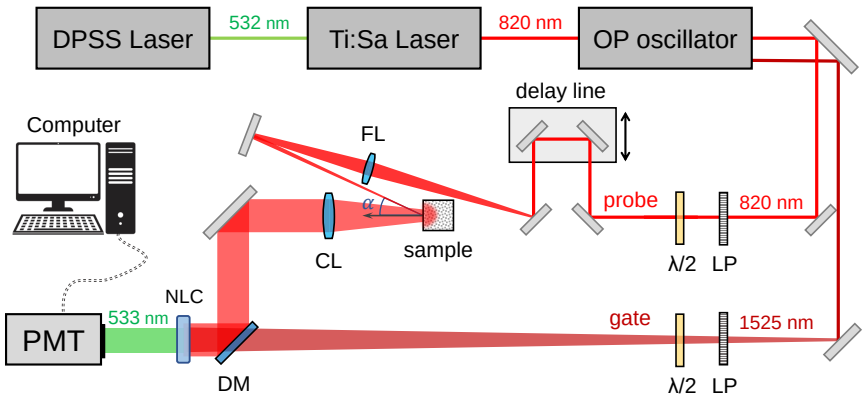

Figure 1: Simplified schematics of the experimental setup for time-resolved measurements. DPSS: Diode-pumped solid-state laser, Ti:Sa: Titanium-Sapphire laser, OP: optical parametric oscillator, LP: linear polarizer, $\lambda/2$: half-wave plate, FL: focusing lens, CL: collection lens, DM: dichroic mirror, NLC: non-linear crystal, PMT: photo-multiplier tube.

generating a sum-frequency signal at 533 nm proportional to the cross-correlation of the original pulses as a function of the delay-line position. Finally, the up-converted signal is detected by a photo-multiplier tube.

The non-linear crystal conversion is a polarization sensitive process that requires both beams to be linearly polarized in the same channel, therefore it acts as a polarization filter for detected light. In order to collect the time-resolved intensity in the co-polarized and cross-polarized configurations, two measurements are performed in succession by simply rotating the probe linear polarization by 90°. Assuming that the sample is homogeneous and isotropic, this methods is equivalent to keeping the probe polarization fixed and measuring the two output polarization channels of the signal.

2.2 Monte Carlo simulations

Our experimental measurements are fitted with Monte Carlo (MC) simulations performed with Monte Carlo eXtreme, an open-source software tool that recently implemented polarized light simulations for monodisperse spherical scatterers.[8] A Stokes vector $\boldsymbol{S}_i$ is associated to each simulated trajectory, where i is the trajectory index, and it is updated at every scattering event based on Mie theory, which depends on the wavelength λ, the sphere radius r, and the refractive index contrast $n_{\text{sph}}/n_{\text{env}}$ between the spheres and the host environment. Unless specified otherwise, each simulation comprises 10^7 trajectories, all set in a initial polarization state:

$$\boldsymbol{S}^{\text{in}} = \begin{pmatrix} I \\ Q \\ U \\ V \end{pmatrix} = \begin{pmatrix} 1 \\ -1 \\ 0 \\ 0 \end{pmatrix}, \tag{6}$$

which corresponds to a vertical linear polarization along the y axis. Three output quantities are associated to each detected trajectory: the exit time t_i^{out}, the exit angles (θ_i, ϕ_i) and the final Stokes vector $\boldsymbol{S}_i^{\text{out}}$. The Stokes vectors are handled and updated in the trajectory reference frame. A conversion to the laboratory reference frame is finally performed based on their azimuthal exit angle ϕ_i via a simple rotation $\boldsymbol{R}(\phi_i)$:

$$\boldsymbol{S}_i^{\text{lab}} = \begin{pmatrix} I_i' \\ Q_i' \\ U_i' \\ V_i' \end{pmatrix} = \boldsymbol{R}(\phi_i)\boldsymbol{S}_i^{\text{out}} = \begin{pmatrix} I_i \\ Q_i \cos(2\phi_i) \\ U_i \sin(2\phi_i) \\ V_i \end{pmatrix}. \tag{7}$$

The co-polarized (y) and cross-polarized (x) intensity projections are therefore evaluated for each trajectory

as:

$$I_{\parallel,i} = |E_{y,i}|^2 = \frac{I'_i + Q'_i}{2} \tag{8}$$

$$I_{\perp,i} = |E_{x,i}|^2 = \frac{I'_i - Q'_i}{2}. \tag{9}$$

To produce the time-resolved curves a weighted histogram method is implemented. The back-scattered trajectories are binned by their exit times with a weight proportional to their intensity projections, to obtain the corresponding time-resolved intensity in the two polarization channels: $I_{\parallel}(t)$, $I_{\perp}(t)$. It should be noted that at the moment, MCX does not update the Stokes vectors when the trajectories interact with an index mismatch boundary. We estimate that the relative error introduced in this case should not exceed a few percent, depending on the refractive index contrast between the sample and its environment.

3. EXPERIMENTAL RESULTS

As an illustrative example of our time-domain depolarization analysis, we report on a depolarization measurements on *Intralipid* 10 % emulsion, and their analysis using polarized MC simulations. *Intralipid* is a lipid emulsion routinely used for parenteral nutrition which has been often used in literature as a scattering phantom or calibration standard due to its high stability and reproducibility. For this reason, its optical properties have been characterized several times by multiple groups through inter-laboratory using different techniques. It is composed of 10 % volume of soybean oil in water, and some other minor ingredients. *Intralipid* is a polydispersion, comprising a broad distribution of soybean oil droplets with different sizes and an average value $\langle r \rangle$. In the following, we assume a refractive index of $n_{\mathrm{sph}} = 1.47$ for the soybean oil spheres and $n_{\mathrm{env}} = 1.33$ for the water. The effective refractive index and the absorption rate of the overall emulsion does not differ significantly from that of water.

A few centiliters of the emulsion were poured in a cuvette made of optical polystyrene with 1.1 mm-thick walls and $10 \times 10 \times 100\,\mathrm{mm}^3$ internal volume. Figure 2a shows the results of co-polarized and cross-polarized time-resolved reflectance measurements recorded by focusing the probe beam at the center of one of the cuvette facets. The measured intensity curves $I_{\parallel}(t)$, $I_{\perp}(t)$ very rapidly before eventually converging to the same decay after $t \sim 11$ ps, just before time when the first internal reflection inside the cuvette wall is expected. For these reasons, we limit our analysis to the first 9 ps. At such short times the effects of absorption can be safely neglected.

Using Eq. (5) we fitted the resulting δ_{R} curve between $2\,\mathrm{ps} < t < 6\,\mathrm{ps}$ (Fig. 2b) to retrieve the depolarization time and the corresponding depolarization length $l_{\mathrm{p}} = (390 \pm 30)\,\mu\mathrm{m}$. The transport mean free path was determined independently by measuring the transverse spread rate through a reflection transient imaging technique,[9,10] returning $l_{\mathrm{t}} = (168 \pm 7)\,\mu\mathrm{m}$.

The resulting data were finally compared with a series of polarized Monte Carlo simulations in order to retrieve the best matching average particle radius r. Despite the monodisperse simplification applied in the numerical model, the simulation results are found in good agreement with the time-resolved CoP and CrP intensities, and in excellent agreement when compared to the δ_{R} decay. The retrieved particle radius is $\langle r \rangle = (140 \pm 15)\,\mathrm{nm}$, corresponding to an asymmetry factor of $g = (0.36 \pm 0.07)$, which agrees well with previous reports on the same sample.[11] The scatterers in the emulsion exhibit a broad distribution of radii spanning from 10 nm to 350 nm, hindering the accurate determination of its average value, which depends on the measurement technique.[12] However, the average value obtained with our method falls well within the expected range, despite having considered only a single particle radius in our numerical simulations.

4. DISCUSSION

Steady-state depolarization studies are often considered in the literature as an important tool for medical diagnostics and material characterization. Our experimental analysis confirms that their utility increases significantly by looking at the time evolution of the depolarization signal. In particular, the depolarization length of a scattering sample can be readily accessed exploiting the intrinsic polarization sensitivity of an all-optical gating technique, granting the sub-ps time resolution needed to detect the fast depolarization dynamics which characterizes even

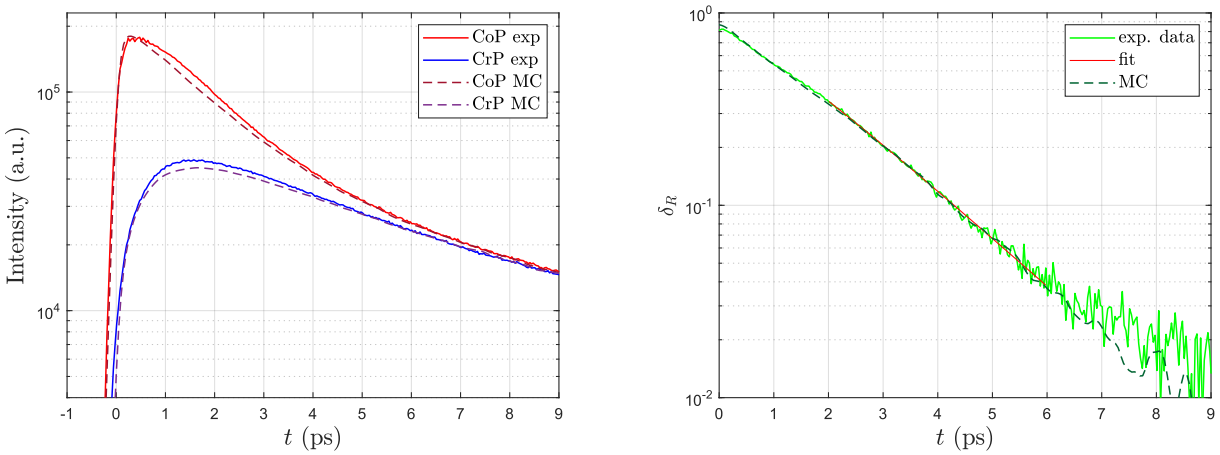

(a) (b)

Figure 2: (a) Time-resolved intensity measurements for the co-polarized and cross-polarized configurations. (b) Time-resolved Depolarization Ratio for Intralipid emulsion fitted with Eq. (5) (solid, red) to retrieve l_{p}. Dashed lines represent the best-fit Monte Carlo simulation obtained with $l_{\mathrm{t}} = 168\,\mu\mathrm{m}$, $r = 140\,\mathrm{nm}$, $\lambda = 820\,\mathrm{nm}$.

moderately turbid materials. We envision that analyzing the time-domain behavior of depolarization curves can provide useful and robust information down to the level of single scattering events that would be difficult to retrieve otherwise, as we demonstrated practically in a simple particle sizing application.

ACKNOWLEDGMENTS

E.P. acknowledges financial support from SONY corporation. L.P. acknowledges financial support by the European Union's NextGenerationEU Programme through the I-PHOQS Research Infrastructure [IR0000016, ID D2B8D520, CUP B53C22001750006] "Integrated infrastructure initiative in Photonic and Quantum Sciences", and NVIDIA Corporation for the donation of the Titan X Pascal GPU used for this research. E.P. and L.P. wishes to thank Prof. Jessica Ramella-Roman and Prof. Min Xu for discussions and help. L.P. and E.P. acknowledge the CINECA award under the ISCRA initiative (project: ARTTESC), for the availability of high-performance computing resources and support.

REFERENCES

[1] Vreeker, R., Van Albada, M., Sprik, R., and Lagendijk, A., "Depolarization of femtosecond laser pulses in disordered media," *Optics communications* **70**(5), 365–368 (1989).

[2] Yoo, K. and Alfano, R., "Time resolved depolarization of multiple backscattered light from random media," *Physics letters A* **142**(8-9), 531–536 (1989).

[3] Dogariu, A., Kutsche, C., Likamwa, P., Boreman, G., and Moudgil, B., "Time-domain depolarization of waves retroreflected from dense colloidal media," *Optics letters* **22**(9), 585–587 (1997).

[4] Doronin, A., Tchvialeva, L., Markhvida, I., Lee, T. K., and Meglinski, I., "Backscattering of linearly polarized light from turbid tissue-like scattering medium with rough surface," *Journal of biomedical optics* **21**(7), 071117–071117 (2016).

[5] Lopushenko, I., Sieryi, O., Bykov, A., and Meglinski, I., "Exploring the evolution of circular polarized light backscattered from turbid tissue-like disperse medium utilizing generalized monte carlo modeling approach with a combined use of jones and stokes–mueller formalisms," *Journal of Biomedical Optics* **29**(5), 052913–052913 (2024).

[6] Rojas-Ochoa, L. F., Lacoste, D., Lenke, R., Schurtenberger, P., and Scheffold, F., "Depolarization of backscattered linearly polarized light," *JOSA A* **21**(9), 1799–1804 (2004).

[7] Xu, M. and Alfano, R. R., "Random walk of polarized light in turbid media," *Physical review letters* **95**(21), 213901 (2005).

[8] Yan, S., Jacques, S. L., Ramella-Roman, J. C., and Fang, Q., "Graphics-processing-unit-accelerated monte carlo simulation of polarized light in complex three-dimensional media," *Journal of Biomedical Optics* **27**(8), 083015–083015 (2022).

[9] Pattelli, L., Savo, R., Burresi, M., and Wiersma, D. S., "Spatio-temporal visualization of light transport in complex photonic structures," *Light: Science & Applications* **5**(5), e16090–e16090 (2016).

[10] Pini, E., Mazzamuto, G., Riboli, F., Wiersma, D. S., and Pattelli, L., "Breakdown of self-similarity in light transport," *arXiv preprint arXiv:2304.02773* (2023).

[11] Michels, R., Foschum, F., and Kienle, A., "Optical properties of fat emulsions," *Optics express* **16**(8), 5907–5925 (2008).

[12] Kodach, V., Faber, D., Van Marle, J., Van Leeuwen, T., and Kalkman, J., "Determination of the scattering anisotropy with optical coherence tomography," *Optics express* **19**(7), 6131–6140 (2011).